The structure of the Au$_3$Pd(113) surface studied by low energy ion scattering

M. Aschoff *, G. Piaszenski, S. Speller, W. Heiland

University of Osnabrück, D-49069 Osnabrück, Germany

Abstract

The structure of the Au$_3$Pd(113) surface has been studied by low energy ion scattering. The surface is not bulk terminated. The top [1$\bar{1}$0] rows are formed by Au atoms. Pd is found in the second layer only. The distance between the first and second layer is reduced by approximately 25% compared to the bulk interplanar distance. © 1998 Elsevier Science B.V. All rights reserved.

Keywords: Alloys; Gold; Low energy ion scattering (LEIS); Palladium; Surface structure, morphology, roughness, and topography

1. Introduction

Metal alloy surfaces find increasing interest in surface science research. In the case of AuPd alloys one reason for studying its surface properties is the application in HF-connectors [1]. So far no study of AuPd single crystal surfaces has been published. Other alloy surfaces have been found greater interest. This paper is not the place to review all this work. We restrict ourselves to listing the more recent studies using low energy ion scattering as a surface analytical tool. These are all fcc metal alloys, as AuPd, e.g. Cu$_3$Pt(111) [2], Ni$_3$Al(100) and (110) [3] and Au containing alloys like Cu$_3$Au(110) [4], Cu$_3$Au(100) [4,5] and Au$_3$Cu(001) [6]. All Au containing alloys show segregation of Au to the surface [4–6]. On the Cu$_3$Au(100) surface an interesting rippling effect has been observed [5]. Previous work on alloys using low energy ion scattering methods has been summarized recently [7].

* Corresponding author.

2. Experiment and results

For the ion scattering experiments we used a UHV system described in detail elsewhere [8]. The ions were produced in a plasma source, accelerated, mass analysed and focused on the target. The source was operated between 200 eV and 15 keV. For the present study we used 1.5 keV He for the surface composition analysis and 2.0 keV Ne ions for the structure analysis. For the composition analysis the energy of the scattered ions was measured with an electrostatic energy analyser (LEIS [7]). For the structure analysis the primary beam was pulsed and the scattered ions were measured using a time-of-flight (TOF) system at a scattering angle of 165° (NICISS-mode [7]). Fig. 1 shows the result of an azimuthal scan in the NICISS-mode defining the crystallographic surface directions. It took long sputter and annealing cycles before a satisfactory azimuthal scan, i.e. a low minimum yield for the [1$\bar{1}$0] direction, was obtained. The azimuthal scan is a real space
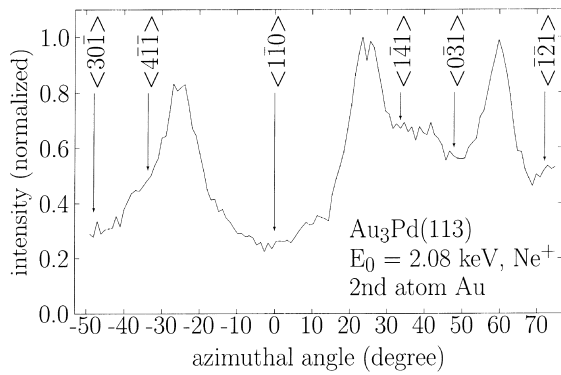
Fig. 1. NICISS azimuthal scan with 2.08 keV Ne on Au₃Pd(113). The angle of incidence is 11°, the laboratory scattering angle is 165°.

representation of the surface crystallographic structure. The broad minimum at $\phi = 0°$ can be identified with the surface half-channels formed by the [1$\bar{1}$0] surface rows. The parallel observation of the LEED pattern agreed with the qualitative NICISS analysis. Fig. 2 gives a model of the Au₃Pd(113) surface. Comparing this model with the azimuthal scan of Fig. 1, the other minima can be identified as given in Fig. 1 by their respective angular positions.

The first structural analyses were NICISS experiments, where the azimuthal angle was fixed along the [1$\bar{1}$0] direction and the angle of incidence was varied [9]. The results, as described in detail in Ref. [9], show that the top [1$\bar{1}$0] rows contain no Pd atoms. Pd is found in the second layer only. The surface lattice constant of the Au rows is at
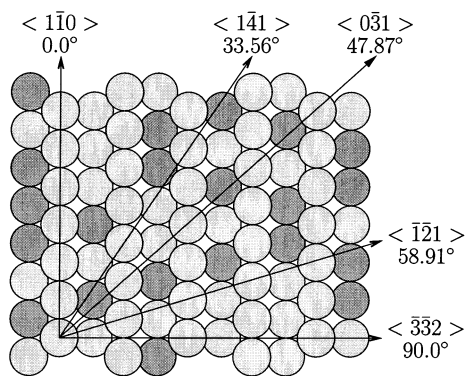

Fig. 2. Model of the Au₃Pd(113) surface, light atoms are Au, shaded atoms are Pd.

2.81 ± 0.05 Å marginally smaller than that for [1$\bar{1}$0] on a Au(110) surface, 2.88 Å, and also smaller than the value expected for Au₃Pd, 2.85 Å [10]. The surface atom thermal vibrations of Au and Pd correspond to Debye temperatures of 80 and 73 K, respectively. The NICISS results give evidence that the second layer rows are disordered. These findings are qualitatively presented in the model of Fig. 2.

In the following the NICISS data for the [0$\bar{3}$1] and the [1$\bar{2}$1] directions will be discussed. These directions are characterized by minima in the azimuthal scan (Fig. 1) due to their semi-channel structure like the [1$\bar{1}$0] semi-channel. Figs. 3 and 4 are the survey impact angle scans for both the Au and the Pd peak of the respective TOF spectra. Note that in the case of Ne scattering from Au₃Pd the peaks corresponding to scattering from Au and Pd, respectively, are well separated. These scans show clearly that there are no Pd atoms in the top layer, because the "first" peak at an angle of incidence of 14° is missing. The intensity increase at small angles of incidence (grazing incidence) corresponds to the scattering from top row atoms [7]. The following peaks, for larger angles of incidence, involve the scattering from second or third layer atoms. In Fig. 5 the atomic positions along the [0$\bar{3}$1] direction of a (113) fcc surface are
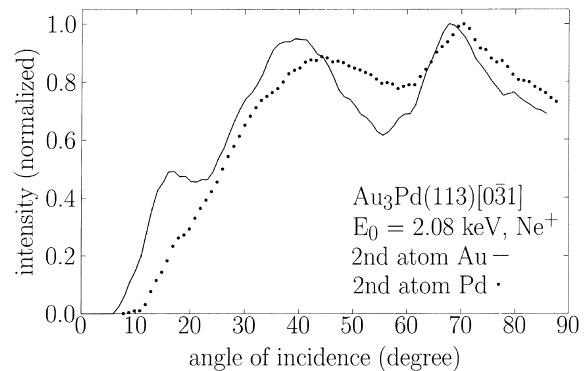

Fig. 3. NICISS "polar" scan for the [0$\bar{3}$1] surface direction of Au₃Pd(113) with Ne at 2.08 keV. The solid line is for backscattering from Au as the second atom and the dotted line for Pd as the second atom. Note that under these conditions a double scattering experiment is performed, the first atom causes a small angle deflection, < 5°, the second atom leads to a large deflection, > 160°. The total scattering angle is 165°.
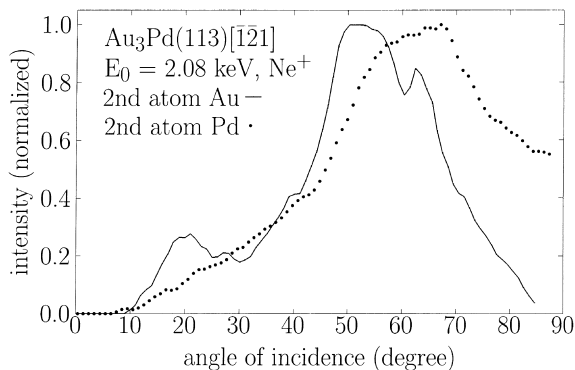
Fig. 4. As in Fig. 2 for the $[\bar{1}\bar{2}1]$ surface direction.

Fig. 6. Comparison of the experimental data (dots) with the result of a two-atom model calculation (solid line). The fit is limited from $8°$ to $18°$. In these limits the rms deviation is 0.03%.

shown. The peaks in Fig. 3 arise from the scattering involving pairs of atoms, e.g. 3–7, 7–11, etc. which give rise to the "first" peak at a critical angle of $14°$. We define the critical angle at approximately 90% of the peak intensity. The second peak, at a critical angle of approximately $31°$, is due to scattering of atom pairs, e.g. 3–5, 7–9, etc. The "last" peak at $62°$ is very likely due to focusing effects from first layer atoms down to the fourth layer, e.g. 3–6, 7–10, etc. From the angular distance between the "first" ($14°$) and "second" ($31°$) peak, the interplanar distance d_{12} can be evaluated. We find $d_{12}=0.9$ Å or a contraction of 25% compared to the bulk value. A contraction of this size was observed in case of e.g. Au(110) (1×2) [11]. The $[\bar{1}\bar{2}1]$ data (Fig. 4) lead to identical results, so we show no further details here. In Fig. 6 the best fit for the first $[0\bar{3}1]$ Au peak is shown. The parameters established by the fit are in agreement with the lattice constant as found from the $[1\bar{1}0]$ direction. The surface thermal vibrational amplitudes are larger corresponding to lower Debye temperatures. This is expected for higher index surface directions [12]. The results indicate no buckling or rippling of the $[1\bar{1}0]$ rows. There is no
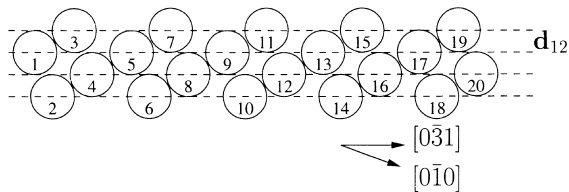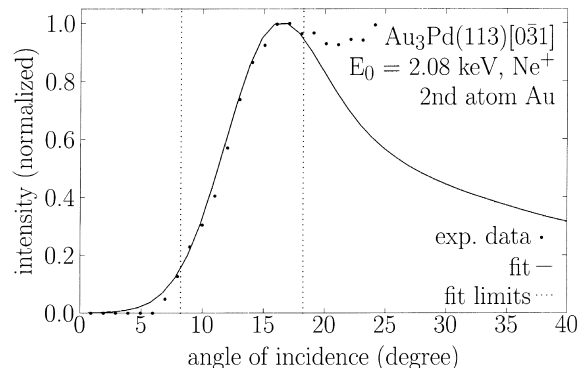
evidence for the presence of vacancies in the surface. NICISS is sensitive to vacancies at a level of approximately 5% [7,11,13]. The calculated results agree with the experiments at a level of $<0.15\%$ (rms).

The calculations use a "two-atom" scattering model [11,14]. The scattering potential is a screened Coulomb potential (Ziegler–Biersack–Littmark [15]). The method is based on the shadow cone effect, i.e. each atom in a given row on a surface forms a shadow cone. At small grazing angles none of the neighbouring atoms are hit under an impact parameter small enough to cause scattering into a large scattering angle. Under these conditions surface channeling prevails. With increasing angle of incidence the neighbouring atoms are brought to the edge of the shadow cone. At the edge of the shadow cone the ion flux is enhanced. This is the cause of the intensity maxima in the experimental and calculated data (Figs. 3–5).

3. Summary

Using low energy ion scattering in the NICISS-mode (neutral impact collision ion scattering spectrometry) we have determined structural parameters of the Au$_3$Pd(113) surface. The surface is not bulk terminated. The top $[1\bar{1}0]$ rows contain Au atoms only. The second layer $[1\bar{1}0]$ contain Pd and Au, but probably these rows are disordered.

Fig. 5. Model of the $[0\bar{3}1]$ direction of Au$_3$Pd(113) (side view).

The lattice parameter of the [1$\bar{1}$0] rows is smaller than the expected bulk value. The interplanar distance between the first and second layer is reduced by approximately 25% compared to the bulk value.

Acknowledgements

References

[1] E.J. Kudrak, J.A. Abys, Intercom. Tech. 28 (1993) 18.
[2] Y.G. Shen, D.J. O'Connor, K. Wandelt, R.J. MacDonald, Surf. Sci. 328 (1995) 21.
[3] Y.G. Shen, D.J. O'Connor, R.J. MacDonald, K. Wandelt, in: R.J. MacDonald, E.C. Taglauer, K.R. Wandelt (Eds.), Surface Science, Springer, Berlin, 1996, p. 115.
[4] H. Niehus, Phys. Status Solidi B 192 (1995) 357.
[5] L. Houssiau, P. Bertrand, Nucl. Instrum. Meth. B 125 (1997) 328.
[6] S. Schömann, E. Taglauer, Surf. Rev. Lett., in press.
[7] H. Niehus, W. Heiland, E. Taglauer, Surf. Sci. Rep. 17 (1993) 213.
[8] J. Möller, H. Niehus, K.J. Snowdon, W. Heiland, Surf. Sci. 178 (1986) 475.
[9] G. Piaszenski, M. Aschoff, S. Speller, W. Heiland, Nucl. Instrum. Meth. B 315 (1998) 331.
[10] M. Hansen, Constitution of Binary Alloys, McGraw-Hill, New York, 1958.
[11] E. van de Riet, H. Derks, W. Heiland, Surf. Sci. 234 (1990) 53.
[12] D.P. Jackson, Surf. Sci. 43 (1974) 431.
[13] S. Speller, M. Schleberger, A. Niehof, W. Heiland, Phys. Rev. Lett. 68 (1992) 3452.
[14] E. van de Riet, J.M. Fluit, A. Niehaus, Surf. Sci. 231 (1990) 368.
[15] J.F. Ziegler, J.P. Biersack, U. Littmark, The Stopping and Range of Ions in Solids, Vol. 1, Pergamon, New York, 1985.